

## NCOA4 maintains murine erythropoiesis via cell autonomous and non-autonomous mechanisms

Naiara Santana-Codina,<sup>1,\*</sup> Sebastian Gableske,<sup>1,\*</sup> Maria Quiles del Rey,<sup>1</sup> Beata Małachowska,<sup>2,3</sup> Mark P. Jedrychowski,<sup>1,4</sup> Douglas E. Biancur,<sup>1</sup> Paul J. Schmidt,<sup>5</sup> Mark D. Fleming,<sup>5</sup> Wojciech Fendler,<sup>1,2</sup> J. Wade Harper,<sup>4,#</sup> Alec C. Kimmelman<sup>6,#</sup> and Joseph D. Mancias<sup>1</sup>

<sup>1</sup>Division of Genomic Stability and DNA Repair, Department of Radiation Oncology, Dana-Farber Cancer Institute, Boston, MA, USA; <sup>2</sup>Department of Biostatistics and Translational Medicine, Medical University of Lodz, Poland; <sup>3</sup>Postgraduate School of Molecular Medicine, Medical University of Warsaw, Poland; <sup>4</sup>Department of Cell Biology, Harvard Medical School, Boston, MA, USA; <sup>5</sup>Department of Pathology, Boston Children's Hospital and Harvard Medical School, Boston, MA, USA and <sup>6</sup>Department of Radiation Oncology, Perlmutter Cancer Center, New York University School of Medicine, New York, NY, USA

\* *These authors contributed equally to this work*

©2019 Ferrata Storti Foundation. This is an open-access paper. doi:10.3324/haematol.2018.204123

Received: August 10, 2018.

Accepted: January 9, 2019.

Pre-published: January 10, 2019.

Correspondence: JOSEPH D. MANCIAS - joseph\_mancias@dfci.harvard.edu

---

## SUPPLEMENTARY INFORMATION

### SUPPLEMENTAL EXPERIMENTAL PROCEDURES

**Cell culture.** Cells were cultured in a humidified incubator at 37°C and 5% carbon dioxide (CO<sub>2</sub>). HEK-293T and K562 cell lines were obtained from the American Type Culture Collection (ATCC, Manassas, Virginia) and tested for mycoplasma contamination by PCR. Cells were grown in DMEM (HEK-293T, Life Technologies, 11965) or IMDM (K562, Thermo Fisher 12440053) with 10% FBS and 1% Pen/Strep (Life Technologies 15140). Cell lines were maintained in a centralized bank and authenticated by assessment of cell morphology as well as STR fingerprinting.

**Mouse models and analysis.** The *Ncoa4<sup>fl/fl</sup>* mouse model was generated by Cyagen in a C57BL/6N and C57BL/6J mixed background. A targeting vector was used to insert lox P sites flanking exons 2 through 6 with positive selection via a Frt-flanked neomycin selection cassette. *Ncoa4<sup>fl/fl</sup>* mice were generated after mating with a Flp deleter mouse. *Ncoa4<sup>fl/fl</sup>* mice were then crossed to *B6.Cg<sup>Tg(UBC-cre/ERT2)1Ejb/2J</sup>* mice from the Jackson Laboratory to generate a tamoxifen-inducible *Ncoa4<sup>rec</sup>* mouse. *Ncoa4<sup>fl/fl</sup>* mice were crossed to the *B6.Epor<sup>tm1(EGFP/cre)Uk</sup>* allele<sup>1</sup> to generate a constitutive *Ncoa4<sup>fl/fl</sup>;EpoR-Cre* mouse model. Mice were maintained on the Prolab Isopro RMH diet (Lab Diet; 380 ppm iron). For induction of *Ncoa4* recombination in the *Ncoa4<sup>fl/fl</sup>;UBC-cre/ERT2* model, mice were dosed with 200 mg/kg tamoxifen via oral gavage (Sigma, T56548, 20 mg/ml in corn oil) once every 24h for 5 consecutive days. For induction of hemolysis, animals were injected with 40 mg/kg phenylhydrazine intraperitoneally (Sigma, 114715, 4 mg/ml solution in sterile saline). All experiments were done in adult mice (more than 8 weeks of age, age matched with the colony) except postnatal bleedings (day 10) under a DFCI IACUC approved protocol (DFCI 15-020).

**PCR genotyping.** Genomic DNA was extracted from spleens of *Ncoa4<sup>fl/fl</sup>* and *Ncoa4<sup>rec</sup>* or sorted Ter119<sup>+</sup> RBC cells from *EpoR-Cre* and *Ncoa4<sup>fl/fl</sup>;EpoR-Cre* mice using the DNA extraction kit (Qiagen, Cat No./ID: 69506). Targeting was determined by PCR using primers flanking the first loxP site: Fw\_1 :TGCTACTGACTTGTTCTTGCTTGAGG, Rv\_1:TGGATCTCTCCTTCCCTTTAGACAGA (Mutant: 470 bp, WT: 342 bp). Cre recombination was determined by PCR using the following primers: Fw\_2:TGGAGACAAGGTCTCAAAACCAATGC and Rv\_1 (Mutant: 540 bp, WT: no band). Routine genotyping was performed by Transnetyx.

**Hematologic and iron parameters.** Blood was drawn by either retro-orbital, submandibular (serial bleedings, 35  $\mu$ l) and collected in EDTA-treated tubes (BD, 365974) for Complete Blood Count (CBC) analysis (Advia 2120i, Children's Hospital Boston, Department of Laboratory Medicine Clinical Core Laboratories). Serum was obtained at endpoint by cardiac puncture and blood collection in Eppendorf tubes, which was clotted for 15-30 min and centrifuged (2000 x g, 10 min, 4C). For reticulocyte counts, blood was mixed in a 1:4 ratio with new methylene blue (EKI 7443) for 15 minutes and smears were made. More than 10 fields per mouse were acquired at 100X and at least 1000 RBCs were counted manually. Reticulocyte % was calculated as the average number of reticulocytes vs. total RBCs. Tissues were collected and tissue non-heme iron concentrations were determined as previously described<sup>2</sup>. Non-heme iron in Ficoll-purified RBCs was measured as previously described<sup>3</sup>. Iron levels in serum were determined using a kit as per manufacturer's instructions (Fisher Scientific/Pointe Scientific 23666320). Erythropoietin (Epo) levels in serum were determined using an ELISA following the manufacturer's instructions (R&D, MEP00B) for mice where enough serum was available. Ftl levels in serum were determined using an ELISA following manufacturer's instructions (Abcam, ab157713). Haptoglobin (Abcam,

Ab157714) and hemopexin (Genway Biotech, GWB-D5D320) levels in serum were quantified using ELISA kits.

**Flow cytometry.** For hematopoietic cell differentiation analyses, bone marrow or spleen cells were isolated and stained with FITC-conjugated anti-Ter119 (BD Biosciences, 557915) and APC Rat Anti-Mouse Cd44 (BD Biosciences, 559250). Briefly, 30,000 cells were resuspended in 150  $\mu$ L PBS 1X/2% FBS (FACS buffer), washed twice with the buffer and stained for 20 min at 4°C with Ter119/Cd44 (1  $\mu$ L in 50  $\mu$ L). Cells were washed twice with FACS buffer and resuspended in 150  $\mu$ L for FACS analysis. Stained cells were analyzed using a Beckman Coulter Cytoflex and differentiation stages were determined based on published methods<sup>4,5</sup>. We plotted Cd44 vs. FSC for the population of Ter119+ cells. Stages were determined based on previous published methods and kept consistent throughout the analysis. Briefly, stage I corresponds to proerythroblasts, stage II includes basophilic and polychromatic erythroblasts, stage III includes orthochromatic erythroblasts, stage IV includes reticulocytes and stage V includes mature red cells.

**Reactive oxygen species measurements.** Unfixed RBCs ( $1 \times 10^6$ ) from *EpoR-Cre* and *Ncoa4<sup>fl/fl</sup>;EpoR-Cre* mice were resuspended in 100  $\mu$ L of PBS with 2% FBS. Resuspended RBCs were incubated with 30  $\mu$ M 2,7-Dichlorofluorescein diacetate (DCFH, Sigma, D6883) for 30 min at 37 °C and 5% CO<sub>2</sub>, followed by sedimentation at 1800 rpm for 1 min. The supernatant was discarded and reactive oxygen species production was induced by treatment and incubation of RBCs either with 0 mM, 0.25 mM, 0.5 mM or 1 mM H<sub>2</sub>O<sub>2</sub>, or 0  $\mu$ M, 50  $\mu$ M, or 100  $\mu$ M phenylhydrazine (PHZ) for 15 min at RT in the dark. After incubating, RBCs were centrifuged at 1800 rpm for 1 min, the supernatant discarded and then resuspended in 400  $\mu$ L PBS with 2% FBS in FACS tubes (Corning, 352054). Cells were analyzed using a Beckman Coulter Cytoflex and Mean Fluorescence Intensity was quantified (MFI).

**Quantitative PCR.** mRNA was isolated using the RNeasy (Qiagen 74104) and RNase-free DNase kits (Qiagen 79254). Reverse transcription was performed with 2 µg of RNA using oligo-dT and MMLB-HP reverse transcriptase (Epicentre). Quantitative RT-PCR was performed using SYBR Green (Applied Biosystems 4367662) in a QuantStudio 7 machine (Thermo Fisher). All reactions were performed in triplicate and *Actb* was used as an internal control. Sequences for primers are as follows: *Actb*\_Fw: 5'-CAA TTC CAT CAT GAA GTG TGA ACGT-3', *Actb*\_Rv: 5'-CTG CTT GCT GAT CCA CAT CTG CT-3', *Hif-2 $\alpha$* \_Fw: 5'-AGC TCA GGG GAG AAC GCC AAG-3', *Hif-2 $\alpha$* \_Rv: 5'-TGG CCA CGC CTG ACA CCT TT-3', *Hamp*\_Fw: 5'-CCT ATC TCC ATC AAC AGA TG-3', *Hamp*\_Rev: 5'-AAC AGA TAC CAC ACT GGG AA-3', *Erfe*\_Fw: 5'- CCA GGC CCC TTT ATC CCA TC-3', *Erfe*\_Rev: 5'-CTG GTG CAG TGC TCC AGA T-3'.

**Western Blot Analysis.** Cells were harvested in ice cold PBS at 80% confluency and lysed in RIPA buffer containing 50 mM TrisHCl pH 7.4, 150 mM NaCl, 2 mM EDTA, 1% NP-40, 0.1% SDS, protease and phosphatase inhibitors (Life Technologies, 78847). Tissues were harvested by excision, frozen in liquid nitrogen and lysed in RIPA buffer containing 1% SDS as well as protease and phosphatase inhibitors. Ficoll-isolated RBCs were collected and lysed in RIPA buffer containing 1% SDS as well as protease and phosphatase inhibitors. Protein concentration was calculated by the bicinchoninic acid (BCA) assay (Thermo Fisher, 23250). 20-40 µg of protein was separated on 4-12% SDS-PAGE gels (Thermo Fisher, NP0322) and transferred to polyvinylidene difluoride (PVDF) or nitrocellulose membranes (Bio-Rad). Membranes were blocked in 5% dry milk in Tris Buffered Saline with 0.1% Tween 20 (TBST 1X). Incubation with primary antibodies was performed at 4°C overnight. Membranes were washed 3 times with TBST 1X, incubated with peroxidase-conjugated secondary antibody for 1 hour and developed using the Enhanced Chemiluminescence (ECL) Detection System (Thermo Fisher, 32209).

**Histology.** Tissues were processed as previously described<sup>18</sup>. Briefly, tissues were fixed overnight in 10% buffered formalin and embedded in paraffin. Tissue sections were deparaffinized in xylene, rehydrated in ethanol and boiled for 15 minutes with a pressure cooker in 10 mmol/L pH 6.0 citrate buffer for antigen retrieval. Slides were incubated in 0.3% hydrogen peroxide (30 min), washed in PBS and blocked in serum for 1 hour. Primary antibody was incubated overnight at 4C, followed by biotin-conjugated secondary antibody and then developed by DAB (Vector labs SK-4100). Slides were counterstained with hematoxylin, dehydrated and mounted in Permount media (SP15-100; Fisher Scientific). Antibodies used for immunostaining are as follows: Fth1 (Cell Signaling D1D4 #4393, 1:500), Cd68 (Abcam ab31630, 1:200). Sections were examined microscopically using a Leica DM2000 light microscope, and five or more representative fields from each slide were analyzed.

**Lentivirus-Mediated shRNAs.** A lentiviral shRNA plasmid clone (pLKO.1) against shNCOA4 and a control against shGFP were obtained from the RNAi Consortium collection. The target sequences and/or RNAi Consortium clone IDs for each shRNA are as follows shNCOA4 #1: 5'-GGCCCAGGAAGTACTTAA-3' (TRCN0000236185) (NCOA4 accession number NM\_001145263.1); and shGFP: 5'-GCAAGCTGACCCTGAAGTTCAT-3' Addgene [Cambridge, MA] plasmid #30323).

**Quantitative Proteomics.** K562 cells expressing shGFP or shNCOA4 shRNAs were treated with or without 25  $\mu$ M Hemin (Sigma 51280) for 72 h and harvested in ice cold PBS. Quantitative mass spectrometry-based proteomics were performed as previously described<sup>6,7</sup>. TMT isobaric reagents were from Thermo Scientific (90406, Life Technologies). Water and organic solvents were from J.T. Baker (Center Valley, PA, USA). Cells were lysed in 2% SDS buffer with 25 mM NaCl, 20 mM HEPES pH 8.8, 5 mM dithiothreitol (DTT, for disulfide bond reduction), 200  $\mu$ M sodium

orthovanadate (New England Biolabs, P0758S), and 1 x Halt<sup>TM</sup> Protease and Phosphatase Inhibitor Cocktail (Life Technologies, 78847) with zirconium oxide beads (Next Advance / MidSci, ZROB05) using a vortexer for 5 min at maximum speed (Tissue Lyser LT, Qiagen). The homogenate was sedimented by centrifugation at 20,000 x g for 5 min at 4 °C. Proteins were alkylated with 14 mM iodoacetamide (I1149 Sigma) (room temperature, 30 min in the dark). Excess iodoacetamide was quenched with 15 mM dithiothreitol (room temperature, 15 min in the dark). Chloroform–methanol precipitation of proteins from cells was performed prior to protease digestion. In brief, four parts neat methanol was added to each sample and vortexed, one part chloroform was added to the sample and vortexed, and three parts water was added to the sample and vortexed. The sample was centrifuged at 10000 rpm for 2 min at room temperature and subsequently washed twice with 100% methanol. Samples were resuspended in 200 mM HEPES pH 8.5 for digestion. Protein concentrations were determined using the bicinchoninic acid (BCA) assay. For each sample, 100 µg of protein was digested overnight with 1:100 protease-to-protein ratio lysyl endopeptidase (129-02541, Wako Chemicals USA, Inc.) followed by trypsin (V5117, Promega) all at 37 °C. Digested peptides were separated from contaminants using 50 mg silica-bonded phase cartridges (WAT054960, Waters) followed by lyophilization using a speedvac concentrator (SAVANT SPD131DDA, Thermo Fisher) overnight. Approximately 50 µg of peptides from each sample were labeled with TMT reagent. Following incubation at room temperature for 1h, the reaction was quenched with hydroxylamine to a final concentration of 0.3% v/v. The TMT-labeled samples were combined at a 1:1:1:1:1:1:1:1:1 ratio. The sample was acidified, vacuum centrifuged to near dryness, and subjected to C18 SPE (EMPORE 2115, Bioanalytical 3M Company). Samples were separated using basic pH reversed-phase HPLC for protein-level analyses and then pooled into 24 fractions. Data were collected using an Orbitrap

Fusion Lumos mass spectrometer (Thermo Fisher Scientific, San Jose, CA, USA) coupled with a Proxeon EASY-nLC 1200 LC pump (Thermo Fisher Scientific). Peptides were separated on a 75  $\mu\text{m}$  inner diameter microcapillary column packed with 35 cm of Accucore C18 resin (2.6  $\mu\text{m}$ , 100  $\text{\AA}$ , ThermoFisher Scientific). Peptides were separated using a 3 hr gradient of 6–27% acetonitrile in 0.125% formic acid with a flow rate of 400 nL/min. Each analysis used an MS<sup>3</sup>-based TMT method as described previously<sup>8</sup>. The data were acquired using a mass range of  $m/z$  350 – 1350, resolution 120,000, AGC target  $1 \times 10^6$ , maximum injection time 100 ms, dynamic exclusion of 120 seconds for the peptide measurements in the Orbitrap. Data dependent MS<sup>2</sup> spectra were acquired in the ion trap with a normalized collision energy (NCE) set at 35%, AGC target set to  $1.8 \times 10^4$  and a maximum injection time of 120 ms. MS<sup>3</sup> scans were acquired in the Orbitrap with a HCD collision energy set to 55%, AGC target set to  $1.5 \times 10^5$ , maximum injection time of 150 ms, resolution at 50,000 and with a maximum synchronous precursor selection (SPS) precursors set to 10. Mass spectra were processed using a Sequest-based in-house software pipeline as described previously<sup>7</sup>. Protein quantitation values were exported for further analysis. Each reporter ion channel was summed across all quantified proteins and normalized assuming equal protein loading of all nine samples.

### **Bioinformatic analysis**

From all identified proteins only the ones with at least 2 peptides identified were subjected to further analysis. If splice variants of proteins were identified, we analyzed the one with the highest expression level. Proteins that were technical contaminants were excluded from the analysis. Proteome data was log<sub>10</sub>-transformed before analysis in order to normalize distribution. Proteins differing between four groups were selected based on one-way analysis of variance (one-way ANOVA). FDRs were calculated for ANOVA p values using the Benjamini-Hochberg procedure.

Pairwise tests were performed for significant ( $p < 0.05$ ,  $FDR < 0.05$ ) peptides. Post-hoc pairwise comparisons (Bonferroni-adjusted t-test for 4 planned comparisons) were used to identify proteins with significant pairwise differences. Afterwards, gene set enrichment analyses were performed<sup>9</sup>. This analysis searches for the locations of peptides associated with a given biological function or pathway within the ranked list of all peptides present in the dataset and calculates an enrichment score depending on the set being globally up- or down-regulated. GSEA has been successfully used for proteomic data<sup>6</sup>, and its reliance on validated and curated biological pathways made it a good tool for identifying processes dysregulated by Ncoa4 silencing. The canonical pathways MSigDB geneset catalogue (c2.cp.v6.0.symbols.gmt) was selected for global gene set analysis. Additionally, we selected pathways of interest (GO Hemoglobin complex, Hallmark Heme synthesis and Biocarta AHSP pathway) in order to validate the a priori hypothesis. NES were used in order to compare gene sets up- or downregulation status between different proteomic data. Further we used a dataset from Gautier et al.<sup>10</sup> that provides proteomic data for 7 erythropoiesis stages: BFU-E (burst forming unit-erythroid) (Prog1), CFU-E (colony forming unit-erythroid) (Prog2), proerythroblast (ProE), basophilic erythroblast (Baso), polychromatic erythroblast (Poly) and orthochromatic erythroblast (Ortho). We performed preranked GSEA analysis of c2cp.v6.0.symbols.gmt genesets with BFU-E (Prog1) as the baseline. Then, we correlated (using a non-parametrical Spearman rank correlation test) NES values from each comparison with the stage of erythropoiesis (we assumed that comparison of Prog2 vs Prog1 is stage 1, ProE vs Prog 1 is stage 2, etc.) and selected those with absolute values of  $\rho > 0.9$ . Further, we selected genesets that correlated best with the stage of erythropoiesis and were significant (NOM  $p < 0.05$ ) at any erythropoiesis stage when compared with Prog1 cells. Data visualization and hierarchical analysis

were performed with MultiExperiment Viewer (Dana-Farber Cancer Institute, Boston, MA, USA) in which Spearman correlation coefficient was used as a metric of distance.

**Chemicals.** Tamoxifen (Sigma, T5648), Phenylhydrazine (Sigma, 114715), Trichloroacetic Acid (Sigma T9159), Disodium-4,7-Diphenyl-1,1—Phenanthroline Disulfonate (Sigma B1375), Thioglycolic Acid (Sigma T6750), Hemin (Sigma 51280), Sodium Orthovanadate (New England Biolabs, P0758S), Halt<sup>TM</sup> Protease And Phosphatase Inhibitor Cocktail (Life Technologies, 78847), Iodoacetamide (Sigma, I1149), Lysyl Endopeptidase (129-02541, Wako Chemicals USA, Inc.), Hydrogen Peroxide Solution (Sigma, H1009), 2,7-Dichlorofluorescein diacetate (Sigma, D6883), Ficoll-Paque Premium (Sigma, GE17-5442-02).

**Statistics** Statistical analysis was done using GraphPad PRISM software. No statistical methods were used to predetermine sample size. For comparisons between two groups, Student's t-test (unpaired, 2-tailed) was performed for all experiments and Student's t-test (unpaired, 1-tailed) was performed in Figure 3C, 4G and Figure 5G (HCT, day 2). Groups were considered different when  $p < 0.05$ .

### **Study approval**

All animal studies were conducted in compliance with ethical regulations approved by the Dana-Farber Cancer Institute Institutional Animal Care and Use Committee (IACUC) under protocol number 15-020.

## SUPPLEMENTARY REFERENCES

1. Heinrich AC, Pelanda R, Klingmüller U. A mouse model for visualization and conditional mutations in the erythroid lineage. *Blood* 2004;104(3):659–666.
2. Cook JD. *Methods in Hematology*. 1980.
3. Connerty H, Briggs A. New method for the determination of whole-blood iron and hemoglobin. *Clin Chem* 1962;8:151–7.
4. Liu J, Zhang J, Ginzburg Y, et al. Quantitative analysis of murine terminal erythroid differentiation in vivo: novel method to study normal and disordered erythropoiesis. *Blood* 2015;121(8):43–50.
5. Chen K, Liu J, Heck S, Chasis JA, An X, Mohandas N. Resolving the distinct stages in erythroid differentiation based on dynamic changes in membrane protein expression during erythropoiesis. *Proc Natl Acad Sci U S A* 2009;106(41):17413–8.
6. Biancur DE, Paulo JA, Małachowska B, et al. Compensatory metabolic networks in pancreatic cancers upon perturbation of glutamine metabolism. *Nat Commun* 2017;(8):15965.
7. Paulo JA, Gaun A, Gygi SP. Global Analysis of Protein Expression and Phosphorylation Levels in Nicotine-Treated Pancreatic Stellate Cells. *J Proteome Res* 2015;14(10):4246–4256.
8. McAlister GC, Nusinow DP, Jedrychowski MP, et al. MultiNotch MS3 enables accurate, sensitive, and multiplexed detection of differential expression across cancer cell line proteomes. *Anal Chem* 2014;86(14):7150–7158.

9. Subramanian P; Mootha, VK; Mukherjee, S; Ebert, BL; Gillette, MA; Paulovich, A; Pomeroy, SL; Golub, TR; Lander, ES; Mesirov, JP. AT. Gene set enrichment analysis: a knowledge-based approach for interpreting genome-wide expression profiles. *Proc Natl Acad Sci U S A* 2005;102(43):15545–15550.
10. Gautier EF, Ducamp S, Leduc M, et al. Comprehensive Proteomic Analysis of Human Erythropoiesis. *Cell Rep* 2016;16(5):1470–1484.

## SUPPLEMENTARY TABLES

**Supplementary Table 1. Complete blood count (CBC) profiling of *Ncoa4<sup>fl/fl</sup>* and *Ncoa4<sup>rec</sup>* male and female mice.**

Males: *Ncoa4<sup>fl/fl</sup>* (n = 4) vs. *Ncoa4<sup>rec</sup>* (n = 4); females: *Ncoa4<sup>fl/fl</sup>* (n = 8) vs. *Ncoa4<sup>rec</sup>* (n = 7), error values represent s.e.m.

	<i>Ncoa4<sup>fl/fl</sup></i>	<i>Ncoa4<sup>rec</sup></i>
RBC (x10 <sup>6</sup> cells/ $\mu$ l)		
Males	8.6 $\pm$ 0.2	7.17 $\pm$ 0.3*
Females	8.9 $\pm$ 0.3	7.9 $\pm$ 0.3*
HGB (g/dl)		
Males	12.4 $\pm$ 0.3	10.3 $\pm$ 0.4**
Females	13.1 $\pm$ 0.4	11.5 $\pm$ 0.4*
HCT (%)		
Males	53.7 $\pm$ 1.4	44.9 $\pm$ 2.1*
Females	55.6 $\pm$ 1.2	49.7 $\pm$ 1.3**
MCH (pg)		
Males	14.4 $\pm$ 0.03	14.3 $\pm$ 0.1
Females	14.6 $\pm$ 0.1	14.5 $\pm$ 0.1
CHr (pg)		
Males	14.7 $\pm$ 0.2	15.3 $\pm$ 0.2*
Females	14.8 $\pm$ 0.2	15.3 $\pm$ 0.2
MCV (fL)		
Males	62.6 $\pm$ 0.1	62.7 $\pm$ 0.8
Females	62.2 $\pm$ 1.0	62.5 $\pm$ 0.7
RDW (%)		
Males	14.1 $\pm$ 0.4	15.3 $\pm$ 0.7
Females	14.0 $\pm$ 0.2	13.9 $\pm$ 0.3
RETIC (x10 <sup>3</sup> cells/ $\mu$ l)		
Males	270 $\pm$ 20.4	325 $\pm$ 75.5
Females	304 $\pm$ 24.7	202.9 $\pm$ 20.3**
WBC (x10 <sup>3</sup> cells/ $\mu$ l)		
Males	7.5 $\pm$ 0.4	7.1 $\pm$ 0.5
Females	4.9 $\pm$ 0.4	3.9 $\pm$ 0.5
PLT (x10 <sup>3</sup> / $\mu$ l)		
Males	783 $\pm$ 51.1	1189 $\pm$ 93.8**
Females	857 $\pm$ 23.2	1207 $\pm$ 108.8**

Statistical comparison was performed using a two-tailed Student's t-test: \*P < 0.05, \*\*P < 0.01.

**Supplementary Table 2. Complete blood count (CBC) profiling of *Ncoa4<sup>fl/fl</sup>* and *Ncoa4<sup>fl/fl</sup>; UBC-Cre-ERT2* basal (UNT, untreated) mice.**

n = 3 mice/group, error values represent s.e.m.

	Basal (UNT)	
	<i>Ncoa4<sup>fl/fl</sup></i>	<i>Ncoa4<sup>fl/fl</sup>; UBC-Cre-ERT2</i>
RBC (x10 <sup>6</sup> cells/ $\mu$ l)	8.9±0.07	9.37±0.06**
HGB (g/dl)	13.5±0.1	13.9±0.1
HCT (%)	58.4±0.6	59.9±0.9
MCH (pg)	15±0.2	14.8±0.15
CHr (pg)	14.9±0.1	14.5±0.1*
MCV (fL)	65.3±0.4	64.0±0.5
RDW (%)	12.6±0.1	12.9±0.3
RETIC (x10 <sup>3</sup> cells/ $\mu$ l)	199±36.8	237±37.6
WBC (x10 <sup>3</sup> cells/ $\mu$ l)	4.3±0.7	5.9±0.5
PLT (x10 <sup>3</sup> / $\mu$ l))	1233±45.6	1288±64.4

Statistical comparison was performed using a two-tailed Student's t-test: \*P < 0.05, \*\*P < 0.01.

**Supplementary Table 3. Complete blood count (CBC) profiling of C57BL/6 and C57BL/6; *UBC-Cre-ERT2* tamoxifen administered (TAM) mice.**

n = 4 mice/group, error values represent s.e.m.

	Post-Tamoxifen (TAM)	
	C57BL/6	C57BL/6; <i>UBC-Cre-ERT2</i>
RBC (x10 <sup>6</sup> cells/ $\mu$ l)	8.72 $\pm$ 0.4	8.42 $\pm$ 0.3
HGB (g/dl)	12.6 $\pm$ 0.4	11.8 $\pm$ 0.6
HCT (%)	56.4 $\pm$ 2.2	53.8 $\pm$ 1.7
MCH (pg)	14.5 $\pm$ 0.06	14 $\pm$ 0.1**
CHr (pg)	15.1 $\pm$ 0.2	15.9 $\pm$ 0.2*
MCV (fL)	64.5 $\pm$ 0.3	64.1 $\pm$ 0.4
RDW (%)	14.3 $\pm$ 0.3	15.7 $\pm$ 0.3*
RETIC (x10 <sup>3</sup> cells/ $\mu$ l)	248 $\pm$ 11.8	364 $\pm$ 13.7***
WBC (x10 <sup>3</sup> cells/ $\mu$ l)	8.4 $\pm$ 0.6	6.2 $\pm$ 0.5*
PLT (x10 <sup>3</sup> / $\mu$ l)	788 $\pm$ 80.3	1232 $\pm$ 88.5**

Statistical comparison was performed using a two-tailed Student's t-test: \*P < 0.05, \*\*P < 0.01, \*\*\*P < 0.001.

**Supplementary Table 4. Complete blood count (CBC) profiling of *Ncoa4<sup>fl/fl</sup>* and *Ncoa4<sup>rec</sup>* after acute *Ncoa4* recombination and treated with PHZ (14 days post-treatment)**

*Ncoa4<sup>fl/fl</sup>* (n = 4) or *Ncoa4<sup>rec</sup>* (n = 3), error values represent s.e.m.

	<i>Ncoa4<sup>fl/fl</sup></i>	<i>Ncoa4<sup>rec</sup></i>
RBC (x10 <sup>6</sup> cells/ $\mu$ l)	8.8 $\pm$ 0.1	8.5 $\pm$ 0.2
HGB (g/dl)	14.5 $\pm$ 0.7	14.0 $\pm$ 0.5
HCT (%)	62.4 $\pm$ 0.9	60.4 $\pm$ 0.8
MCH (pg)	16.9 $\pm$ 0.05	16.7 $\pm$ 0.1
MCV (fL)	71.1 $\pm$ 0.4	71.4 $\pm$ 1.2
RDW (%)	15.4 $\pm$ 0.2	16.6 $\pm$ 0.4*

Statistical comparison was performed using a two-tailed Student's t-test: \*P < 0.05.

**Supplementary Table 5. Complete Blood Count (CBC) profiling of CL57BL/6, *Ncoa4*<sup>fl/fl</sup>, *EpoR-Cre* and *Ncoa4*<sup>fl/fl</sup>;*EpoR-Cre* mice (data included in Figure 4A)**

CL57BL/6 (n = 6), *Ncoa4*<sup>fl/fl</sup> (n = 11), *EpoR-Cre* (n = 19) and *Ncoa4*<sup>fl/fl</sup>;*EpoR-Cre* (n = 21), error values represent s.e.m.

	C57BL/6	<i>Ncoa4</i> <sup>fl/fl</sup>	<i>EpoR-Cre</i>	<i>Ncoa4</i> <sup>fl/fl</sup> ; <i>EpoR-Cre</i>
RBC (x10 <sup>6</sup> cells/ $\mu$ l)	9.4±0.3	9.6±0.1	9.5±0.1	9.5±0.1
HCT (g/dl)	58.7±2.06	59.8±0.9	61.9±0.9	58.5±1.1
HGB (%)	13.7±0.6	14.1±0.2	13.9±0.1	13.0±0.3 <sup>#</sup>
MCH (pg)	14.6±0.15	14.6±0.15	14.6±0.06	13.8±0.09 <sup>s</sup>
CHr (pg)	14.2±0.3	14.3±0.2	14.5±0.05	13.6±0.07 <sup>s</sup>
MCV (fL)	62.5±0.6	61.9±0.6	64.7±0.4	61.6±0.5 <sup>*</sup>
RDW (%)	13.6±0.3	13.7±0.5	13.1±0.1	13.6±0.1
RETIC (x10 <sup>3</sup> cells/ $\mu$ l)	233.3±18.2	220.7±9.9	208.4±9.1	189.9±12.5
PLT (x10 <sup>3</sup> / $\mu$ l))	1301±80.1	1296±58.2	1326±32.7	1322±35.9
WBC (x10 <sup>3</sup> cells/ $\mu$ l)	8.1±1.25	8.4±0.9	6.1±0.4	6.7±0.4

Statistical comparison was performed using a Dunnett's test (*Ncoa4*<sup>fl/fl</sup>;*EpoR-Cre* group as reference) if ANOVA was significant:

\*P<0.05 *EpoR-Cre* vs *Ncoa4*<sup>fl/fl</sup>;*EpoR-Cre*,

<sup>#</sup>P<0.05 *Ncoa4*<sup>fl/fl</sup> vs *Ncoa4*<sup>fl/fl</sup>;*EpoR-Cre* and *EpoR-Cre* vs *Ncoa4*<sup>fl/fl</sup>;*EpoR-Cre*,

<sup>s</sup>P<0.05 C57BL/6 vs *Ncoa4*<sup>fl/fl</sup>;*EpoR-Cre*, *Ncoa4*<sup>fl/fl</sup> vs *Ncoa4*<sup>fl/fl</sup>;*EpoR-Cre*, *EpoR-Cre* vs *Ncoa4*<sup>fl/fl</sup>;*EpoR-Cre*

**Supplementary Table 6. Complete Blood Count (CBC) profiling of *EpoR-Cre* and *Ncoa4<sup>fl/fl</sup>;EpoR-Cre* mice in the post-natal period (day 10) (data included in Figure 4G)**

*EpoR-Cre* (n = 8) and *Ncoa4<sup>fl/fl</sup>;EpoR-Cre* (n = 5), error values represent s.e.m.

	<i>EpoR-Cre</i>	<i>Ncoa4<sup>fl/fl</sup>;EpoR-Cre</i>
RBC (x10 <sup>6</sup> cells/ $\mu$ l)	4.1 $\pm$ 0.2	3.5 $\pm$ 0.3*
HCT (g/dl)	34.8 $\pm$ 1.08	29.6 $\pm$ 2.9*
HGB (%)	8.5 $\pm$ 0.2	6.5 $\pm$ 0.6**
MCH (pg)	20.6 $\pm$ 0.6	17.9 $\pm$ 0.6**
MCV (fL)	85.2 $\pm$ 2.6	84.7 $\pm$ 0.9
RDW (%)	15.8 $\pm$ 0.5	17.1 $\pm$ 0.8

Statistical comparison was performed using a one-tailed Student's t-test: \*P < 0.05, \*\*P < 0.01.

**Supplementary Table 7. Complete blood count profiling of *EpoR-Cre* and *Ncoa4<sup>fl/fl</sup>;EpoR-Cre* mice in PHZ treated conditions**

Number of mice (n) = 4 mice/group, error values represent s.e.m.

	<i>EpoR-Cre</i>	<i>Ncoa4<sup>fl/fl</sup>; EpoR-Cre</i>
RBC (x10 <sup>6</sup> cells/ $\mu$ l) PHZ 7d	6.3 $\pm$ 0.2	6.3 $\pm$ 0.2
HGB (g/dl) PHZ 7d	10.2 $\pm$ 0.3	9.8 $\pm$ 0.4
HCT (%) PHZ 7d	52.3 $\pm$ 1.1	51.6 $\pm$ 2.4
MCH (pg) PHZ 7d	16.2 $\pm$ 0.4	15.6 $\pm$ 0.3
MCV (fL) PHZ 7d	83.6 $\pm$ 2.2	82 $\pm$ 1.1
RDW (%) PHZ 7d	18.4 $\pm$ 1.03	19.7 $\pm$ 0.8
WBC (x10 <sup>3</sup> cells/ $\mu$ l) PHZ 7d	13.2 $\pm$ 1.6	11.7 $\pm$ 1.0

Statistical comparison was performed using a two-tailed Student's t-test

**Supplementary Tables 8-10: Proteomic and GSEA data (see attached excel spreadsheets)**

**Supplementary Table 8**

**Supplementary Table 9**

**Supplementary Table 10**

**Supplementary Table 11. Nucleotide sequences for PCR, qPCR and shRNA based analyses**

Forward (Fw), reverse (Rv) oligonucleotide sequences and short hairpin (sh) target sequences for lentiviral mediated knockdown

Primers (Fw\_1 and Rv\_1) were used to determine successful targeting of the first loxP site, while primers flanking the Cre site (Fw\_2 and Rv\_1) were used to determine successful recombination.

Application	Sequence 5'-3'
<b>PCR</b>	
Fw_1	TGCTACTGACTTGTTCTTGCTTGAGG
Fw_2	TGGAGACAAGGTCTCAAACCAATGC
Rv_1	TGGATCTCTCCTTCCCTTTAGACAGA
<b>qPCR</b>	
Actb Fw	CAATTCCATCATGAAGTGTGAACGT
Actb Rv	CTGCTTGCTGATCCACATCTGCT
Hif-2 $\alpha$ Fw	AGCTCAGGGGAGAACGCCAAG
Hif-2 $\alpha$ Rv	TGGCCACGCCTGACACCTTT
Hamp Fw	CCTATCTCCATCAACAGATG
Hamp Rv	AACAGATACCACACTGGGAA
Erfe Fw	CCAGGCCCTTTATCCCATC
Erfe Rev	CTGGTGCAGTGCTCCAGAT
<b>shRNA</b>	
shGFP	GCAAGCTGACCCTGAAGTTCAT
shNCOA4 #1	GGCCCAGGAAGTATTACTTAA

## SUPPLEMENTARY FIGURE LEGENDS

### Supplementary Figure 1. Generation of conditional *Ncoa4* knockout mouse model

(A) Schematic of conditional *Ncoa4* knockout mouse model. Different sets of primers were used to determine presence of recombination. F1 and R1 were used to determine the WT gene (342 bp) or the floxed allele (470 bp), while F2:R1 were used to determine presence of recombination (540 bp). (B) Decreased *Ncoa4* protein levels after Tamoxifen administration in *Ncoa4<sup>fl/fl</sup>; UBC-Cre/ERT2* mice. Pancreas, brain and liver were analyzed.  $\beta$ -Actin (*Actb*) serves as loading control. (C) Genomic DNA isolated from pancreas and brains of *Ncoa4<sup>fl/fl</sup>* and *Ncoa4<sup>rec</sup>* yields a PCR product at 470 bp when using primers directed at the floxed allele (left panel, see Methods). This band is not detected in *Ncoa4<sup>rec</sup>* mice. Using primers directed at the recombined allele, a PCR product of 540 bp was detected for *Ncoa4<sup>rec</sup>* but not *Ncoa4<sup>fl/fl</sup>* (right panel). (D) Elevated Fth1 staining in kidney, liver, and spleen but not pancreas of *Ncoa4<sup>rec</sup>* mice 11 days after tamoxifen administration initiation. Representative field (20X) of 4 mice/group (scale bar=100  $\mu$ m). (E) Ftl levels in serum of *Ncoa4<sup>fl/fl</sup>* and *Ncoa4<sup>rec</sup>* mice. (n = 3 mice/group, error bars represent s.e.m.). (F) *Hamp* mRNA fold change of *Ncoa4<sup>rec</sup>* but not *Ncoa4<sup>fl/fl</sup>* mice. (n = 3/group, error bars represent s.e.m.). (G) Ter119-Cd44 staining of bone marrow cells isolated from *Ncoa4<sup>fl/fl</sup>* and *Ncoa4<sup>rec</sup>* mice. Differentiation stages of RBCs gating the Ter119+ population representing Cd44-APC staining vs. Forward Scatter (left diagram). Cells within the Ter119+ population were quantified and cells at each stage of differentiation were represented as percentage of total population (n = 4 mice/group, error bars show s.e.m.) For all panels, statistical comparison was performed using a two-tailed Student's t-test: \*P < 0.05, \*\*P < 0.01, \*\*\*P < 0.001.

## Supplementary Figure 2. *Ncoa4* depletion: long-term and stress-erythropoiesis effects

(A) Ter119-Cd44 staining of bone marrow cells isolated from *Ncoa4*<sup>fl/fl</sup> and *Ncoa4*<sup>rec</sup> mice at day 46 after tamoxifen administration initiation. Cells within the Ter119+ population were quantified and cells at each stage of differentiation were represented as percentage of total population. (n = 5 mice/group, error bars represent s.e.m.) (B) No significant change in spleen size of *Ncoa4*<sup>fl/fl</sup> and *Ncoa4*<sup>rec</sup> mice at day 46 (n = 5/group, error bars show s.e.m). (C) Tamoxifen and PHZ administration pattern of *Ncoa4*<sup>fl/fl</sup> and *Ncoa4*<sup>fl/fl</sup>; *Ubc-cre/ERT2* mice. (D) Serial Complete Blood Count (CBC) profiling and reticulocyte quantification of *Ncoa4*<sup>rec</sup> and *Ncoa4*<sup>fl/fl</sup> mice after TAM and PHZ (n = 5 mice/group, error bars represent s.e.m). (E) Representative field (10X) of 5 mice/group (scale bar=200 μm) of hematoxylin-eosin stained spleens from *Ncoa4*<sup>fl/fl</sup> and *Ncoa4*<sup>rec</sup> mice dosed with PHZ. Slides were graded from 1 to 3 (mild, moderate and severe) according to amount of erythrocyte precursors in the red spleen (spleen erythropoiesis). (F) Cd68 staining in liver of *Ncoa4*<sup>fl/fl</sup> and *Ncoa4*<sup>rec</sup> mice (representative field (10X) of 5 mice/group (scale bar=200 μm). Arrows show foci of erythropoiesis. (G) Elevated Fth1 staining in spleen and liver of *Ncoa4*<sup>rec</sup> mice after tamoxifen and PHZ administration. Representative field (20X) of 5 mice/group (scale bar=100 μm). (H) Haptoglobin (Hp) and hemopexin (Hx) levels in serum of *Ncoa4*<sup>fl/fl</sup> (n = 4) versus *Ncoa4*<sup>rec</sup> (n = 5) mice (error bars show s.e.m) after tamoxifen and PHZ. For all panels, statistical comparison was performed using a two-tailed Student's t-test: \*P < 0.05, \*\*P < 0.01, \*\*\*P < 0.001.

## Supplementary Figure 3. Generation and validation of a *Ncoa4*<sup>fl/fl</sup>; *EpoR-Cre* mouse model.

A murine model of erythrocyte specific *Ncoa4* deficiency was generated using a *EpoR-Cre* recombinase-loxP system to generate *Ncoa4*<sup>fl/fl</sup>; *EpoR-Cre* mice (A) Genomic DNA isolated from

Ter119<sup>+</sup>-sorted *EpoR-Cre* and *Ncoa4<sup>fl/fl</sup>; EpoR-Cre* cells yields a PCR product only for *EpoR-Cre* mice at 342 bp when using primers directed at the WT allele (left panel, see Methods). A PCR product at 540 bp was detected in *Ncoa4<sup>fl/fl</sup>; EpoR-Cre* but not in *EpoR-Cre* mice (right panel) **(B)** Genomic DNA isolated from pancreas of *EpoR-Cre* and *Ncoa4<sup>fl/fl</sup>; EpoR-Cre* cells yield a PCR product at *EpoR-Cre* mice at 342 bp when using primers directed at the WT allele (left panel, see Methods). A PCR product at 470 bp was detected in *Ncoa4<sup>fl/fl</sup>; EpoR-Cre* (see Methods). No band was detected for the recombined product. **(C)** No significant change in spleen size of C57BL/6, *Ncoa4<sup>fl/fl</sup>; EpoR-Cre* and *Ncoa4<sup>fl/fl</sup>; EpoR-Cre*. (C57BL/6, n = 2 mice/group, *Ncoa4<sup>fl/fl</sup>*, n = 6 mice/group, *EpoR-Cre*, n = 5 mice/group, *Ncoa4<sup>fl/fl</sup>; EpoR-Cre*, n = 7 mice/group, error bars represent s.e.m). **(D)** Ter119-Cd44 staining of bone marrow cells isolated from *EpoR-Cre* and *Ncoa4<sup>fl/fl</sup>; EpoR-Cre* mice. Cells within the Ter119<sup>+</sup> population were quantified and cells at each stage of differentiation were represented as percentage of total population (n = 4 mice/group, error bars show s.e.m.) **(E)** PHZ administration increases spleen sizes of *EpoR-Cre* and *Ncoa4<sup>fl/fl</sup>; EpoR-Cre* mice when compared to untreated *Ncoa4<sup>fl/fl</sup>; EpoR-Cre* mice (*Ncoa4<sup>fl/fl</sup>; EpoR-Cre* untreated, n = 7 mice/group, *EpoR-Cre*, n = 4 mice/group, *Ncoa4<sup>fl/fl</sup>; EpoR-Cre*, n = 4 mice/group, error bars represent s.e.m.). Data from UNT group is used as reference in Supplementary Figure 3E and Supplementary Figure 4A. **(F)** Ter119-Cd44 staining of bone marrow (left) and spleen (right) cells isolated from PHZ administered *EpoR-Cre* and *Ncoa4<sup>fl/fl</sup>; EpoR-Cre* mice. Cells within the Ter119<sup>+</sup> population were quantified and cells at each stage of differentiation were represented as percentage of total population (n = 4 mice/group, error bars represent s.e.m.). **(G)** Representative field (10X) of 4 mice/group (scale bar=200 μm) of hematoxylin-eosin stained spleens from *EpoR-Cre* and *Ncoa4<sup>fl/fl</sup>; EpoR-Cre* mice. Slides were graded from 1 to 2 (mild and moderate) according to amount of erythrocyte precursors in the red spleen. (spleen erythropoiesis). **(H)** *Hamp* mRNA

fold change of *EpoR-Cre* versus *Ncoa4<sup>fl/fl</sup>;EpoR-Cre* mice. (n = 3/group, error bars represent s.e.m). **(I)** Haptoglobin (Hp) and hemopexin (Hx) levels in serum of *EpoR-Cre* (n = 6) versus *Ncoa4<sup>fl/fl</sup>;EpoR-Cre* (n = 7) mice (error bars show s.e.m.). For all panels, statistical comparison was performed using a two-tailed Student's t-test: \*P < 0.05, \*\*P < 0.01, \*\*\*P < 0.001.

**Supplementary Figure 4. Long-term comparison of *Ncoa4<sup>fl/fl</sup>;EpoR-Cre* mice with *EpoR-Cre* control when challenged with PHZ.**

**(A)** Normalization of spleen size after PHZ administration in the time course experiment (day 11). Untreated mice are used as a reference for normal spleen size as in Supplementary Figure 3E. **(B)** Epo levels in serum of *EpoR-Cre* versus *Ncoa4<sup>fl/fl</sup>;EpoR-Cre* mice. (n = 3/group, error bars represent s.e.m.) **(C)** Ter119-Cd44 staining of bone marrow cells isolated from PHZ administered *EpoR-Cre* and *Ncoa4<sup>fl/fl</sup>;EpoR-Cre* mice. Cells within the Ter119+ population were quantified and cells at each stage of differentiation were represented as percentage of total population (n = 4 mice/group, error bars represent s.e.m.) **(D)** Non-heme iron levels in isolated RBCs (n = 5/group, error bars represent s.e.m.). For all panels, statistical comparison was performed using a two-tailed Student's t-test: \*P < 0.05, \*\*P < 0.01, \*\*\*P < 0.001.

**Supplementary Figure 5. NCOA4 is required for hemoglobin synthesis and differentiation in K562 cells.**

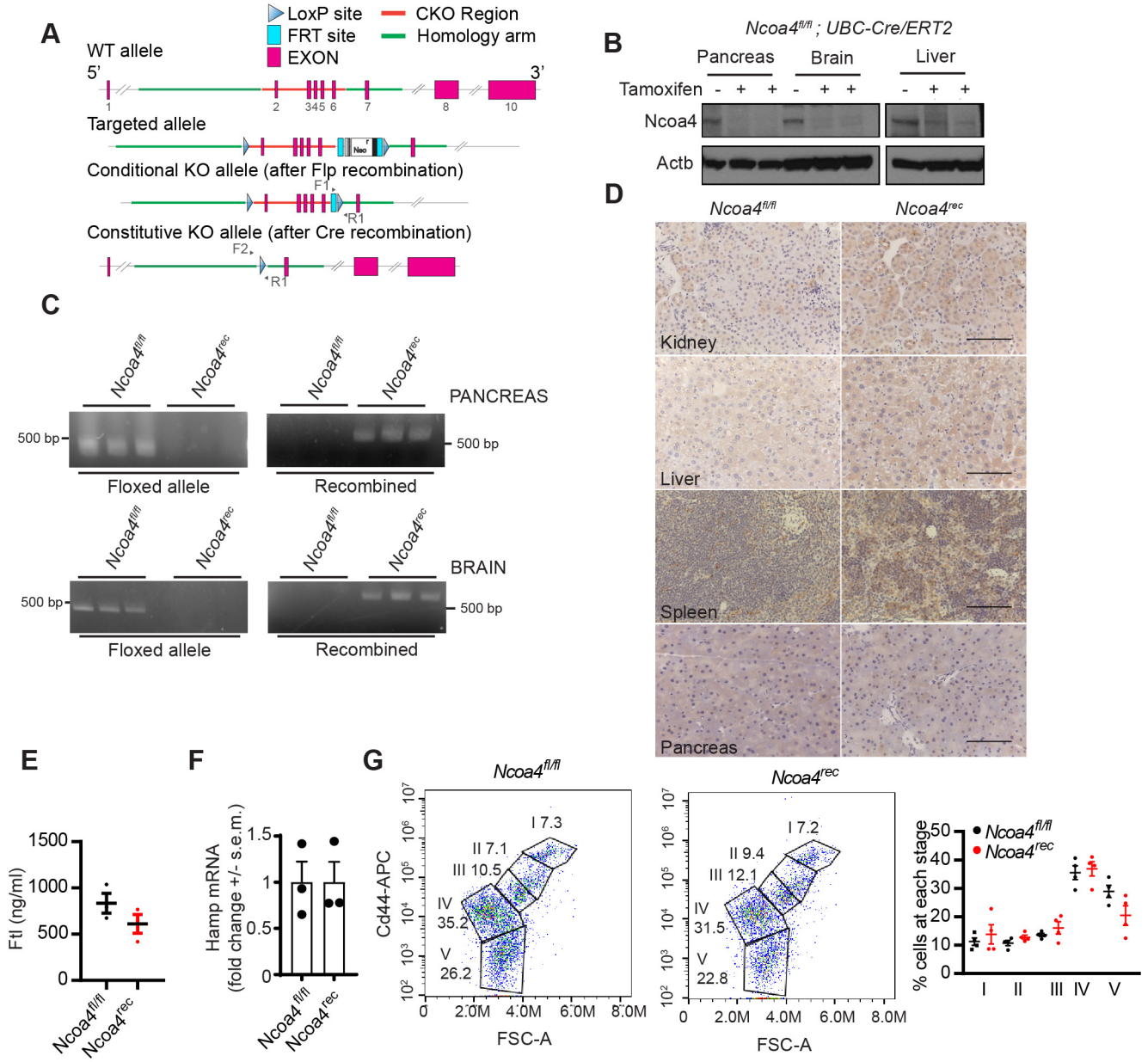
**(A)** Geneset Enrichment analysis results of pathways associated with hemoglobin synthesis pathways (Gene Ontology GO hemoglobin complex, hallmark heme metabolism and Biocarta AHSP pathway). **(B)** Data visualization shows Spearman correlation coefficients of proteomic

profile changes observed between the analyzed groups and differences between erythrocyte maturation stages. Differences of proteomic profiles between: shGFP + Hemin (HM) vs. shGFP, shNCOA4 vs. shGFP, shNCOA4 + HM vs. shGFP + HM and shNCOA4 vs shNcoa4 + HM were correlated with those noted between pairs of: BFU-E (burst forming unit-erythroid) (Prog1), CFU-E (colony forming unit-erythroid) (Prog2), proerythroblast (ProE), basophilic erythroblast (Baso), polychromatic erythroblast (Poly) and orthochromatic erythroblast (Ortho). A positive correlation coefficient indicates grouping between two proteomic data sets whereas a negative value indicates the opposite effect. Details about the analysis are described in the methods section.

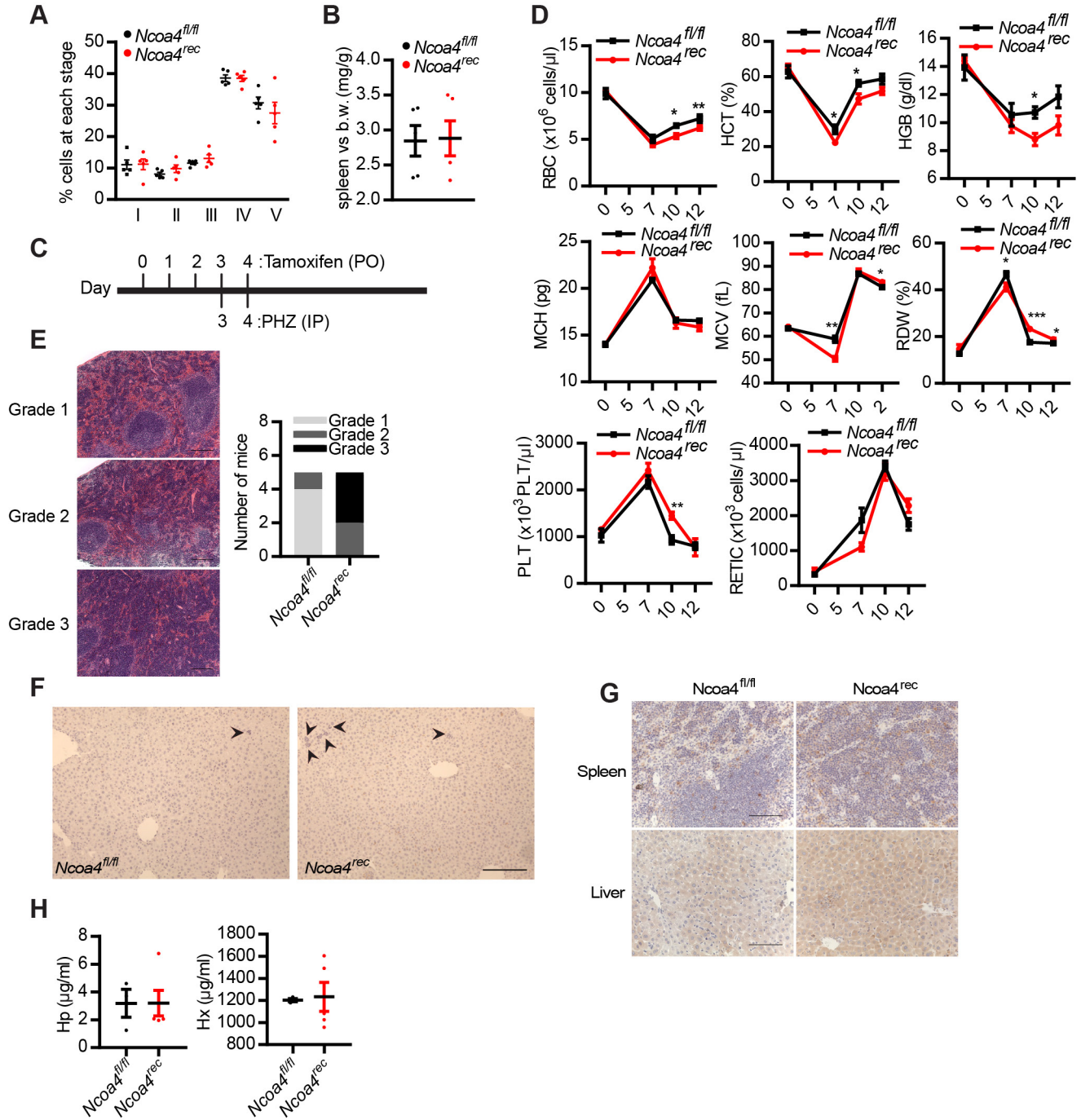
**Supplementary Figure 6. Uncropped immunoblots for all data elements shown in Figures 1-2.**

**Supplementary Figure 7. Uncropped immunoblots for all data elements shown in Figures 3-5 and Supplementary Figure 1B.**

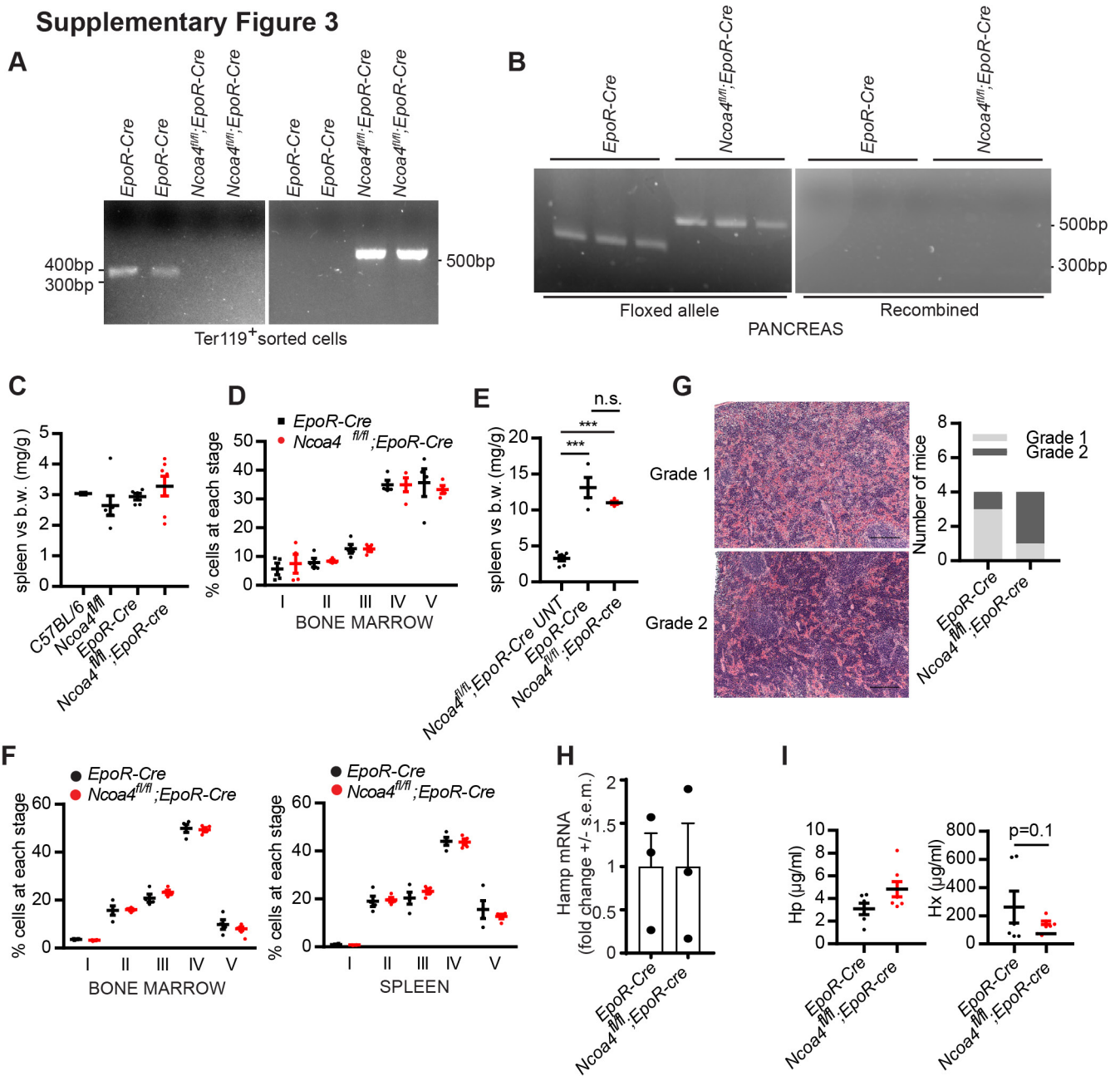
## Supplementary Figure 1



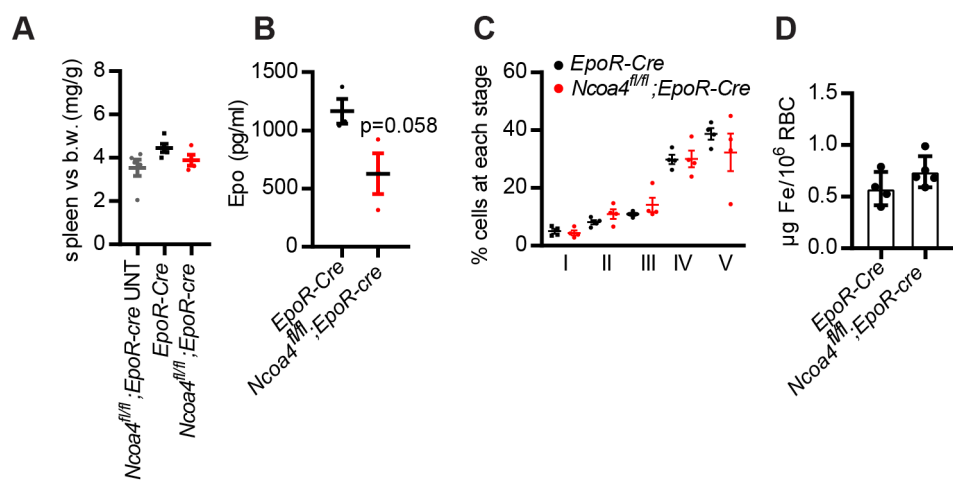
## Supplementary Figure 2



### Supplementary Figure 3

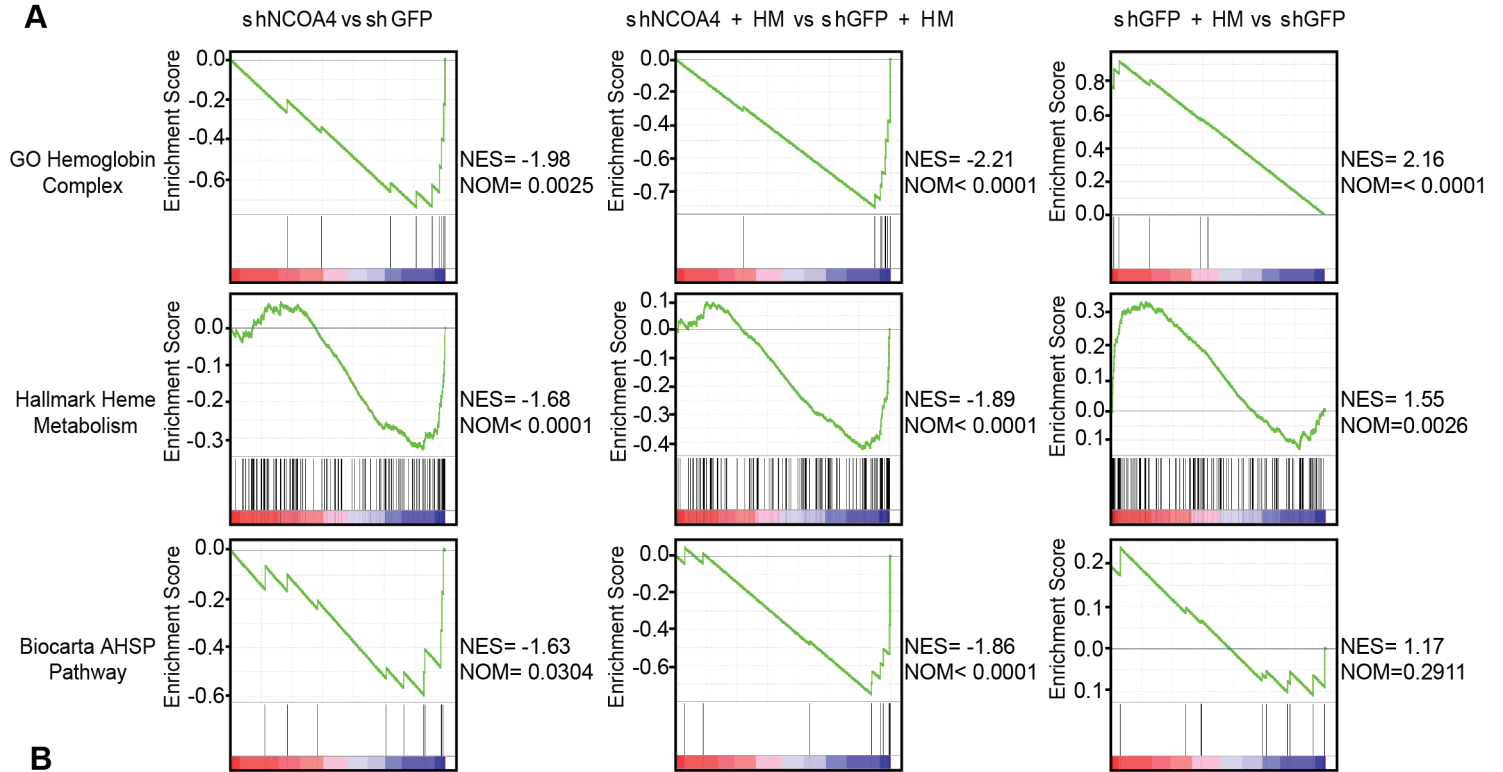


### Supplementary Figure 4

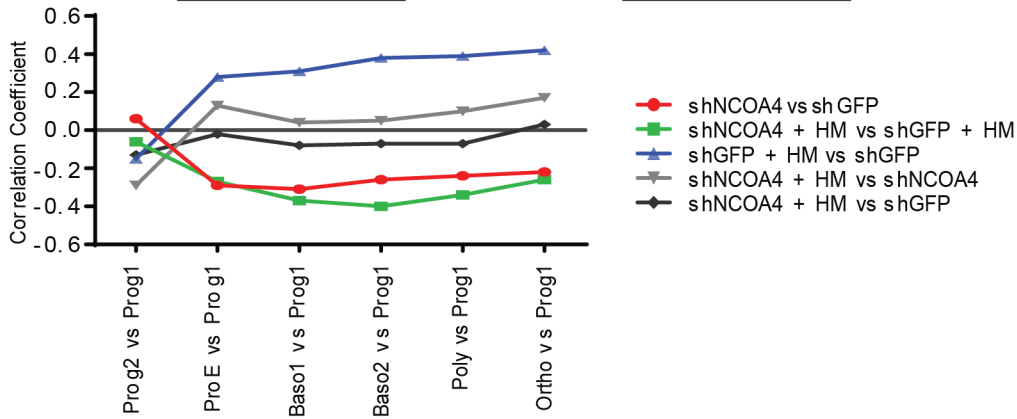


## Supplementary Figure 5

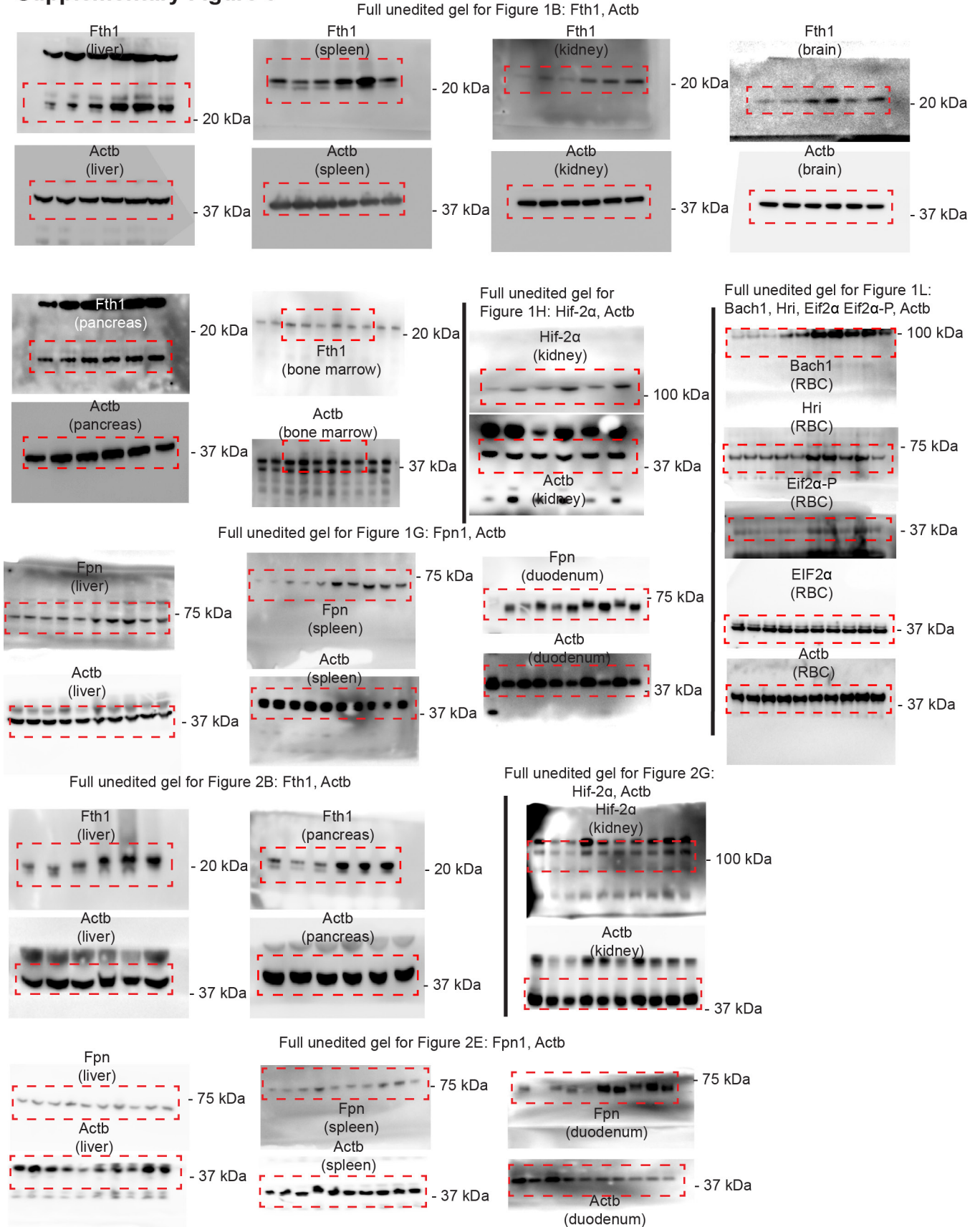
**A**



**B**



# Supplementary Figure 6



## Supplementary Figure 7

